ELSEVIER

Mobility of haloforms on ice surfaces

M.L. Grecea [a,*], E.H.G. Backus [a], H.J. Fraser [b], T. Pradeep [c], A.W. Kleyn [a,d], M. Bonn [a]

[a] *Leiden Institute of Chemistry, University of Leiden, Einsteinweg 55, P.O. Box 9502, 2300 RA Leiden, The Netherlands*
[b] *Raymond & Beverly Sackler Laboratory for Astrophysics, Leiden Observatory, P.O. Box 9513, 2300 RA Leiden, The Netherlands*
[c] *Department of Chemistry and Regional Sophisticated Instrumentation Centre, Indian Institute of Technology Madras, Chennai 600 036, India*
[d] *FOM Institute for Plasma Physics Rijnhuizen, Euratom-FOM Association, P.O. Box 1207, 3430 BE Nieuwegein, The Netherlands*

Abstract

We have investigated the mobility of bromoform ($CHBr_3$) and chloroform ($CHCl_3$) on amorphous solid water and crystalline ice surfaces, by monitoring their adsorption and desorption behavior using temperature programmed desorption spectroscopy and reflection absorption infrared spectroscopy. Up to its desorption temperature, of 140 K, $CHCl_3$ does not diffuse over the crystalline ice surface, whereas $CHBr_3$ is found to be mobile at temperatures as low as 85 K. The results demonstrate distinct differences between the surface mobility of structurally similar haloform molecules on crystalline ice surfaces, which may have implications to the halocarbon chemistry occurring on atmospheric ice particles.
© 2004 Elsevier B.V. All rights reserved.

1. Introduction

In the past decade, halocarbon chemistry in the lower stratosphere has received significant attention, due to its relevance in ozone destruction cycles. Whilst many of the initial investigations have focused on chlorofluorocarbons, the contribution of bromoform ($CHBr_3$) has been increasingly recognized [1], especially given the enhanced ozone destruction potential of bromine in the lower stratosphere [2–4] – two orders of magnitude higher than that of chlorine [2]. Studies of the chemical relevance of atmospheric $CHBr_3$ have received additional impetus with the discovery that algae are a natural source of $CHBr_3$ [5–7], its detection in the lower stratosphere [8,9], and its large number of photodissociation products [10]. The adsorption, desorption and (photo)dissociation dynamics of $CHBr_3$ on ice surfaces are therefore particularly relevant to ozone depletion. In this context, we have investigated the interaction of $CHBr_3$ with ice surfaces and compared it with that of $CHCl_3$.

Adsorption of chloroform on ice has previously been studied by temperature programmed desorption (TPD) spectroscopy [11,12], Fourier transform infrared reflection absorption infrared spectroscopy (FTIRAS) [12] and X-ray photoelectron spectroscopy (XPS) [13]. To the best of our knowledge, bromoform was included in only one IR study on a large series of halomethanes *co-adsorbed* with water ice [14]. Here, we compare the desorption spectra of $CHCl_3$ and $CHBr_3$ dosed on the surfaces of amorphous solid water (ASW) and crystalline ice (CI). The results indicate that, up to the desorption temperature, of 140 K, $CHCl_3$ is immobile on the CI surface, whereas $CHBr_3$ is already mobile at 85 K.

2. Experimental

The experimental setup, described in detail elsewhere [15,16], consists of an UHV chamber with a base pressure of 3×10^{-11} mbar, with a triply differentially pumped compact molecular beam line attached for dosage of water onto a Pt(533) crystal. This substrate is mounted on a liquid nitrogen cooled, temperature-controlled sample holder and its cleanliness was checked using nitrogen monoxide TPD [17]. Water was obtained

---

from a Simplicity Millipore system (resistivity >18 MΩ/cm). Compact non-porous ASW layers were prepared by depositing water from the molecular beam under normal incidence at substrate temperatures of 85 K (at deposition rates of ~6 ML/min). CI layers were obtained by slow annealing of ASW layers. After crystallization of the amorphous layer, the sample was cooled back down to 85 K. The structure of the water layers was confirmed by reflection absorption infrared spectroscopy (RAIRS) [18–20]. Haloform molecules were subsequently adsorbed on the ice surfaces by background dosing of CHBr$_3$ (>99% Sigma-Aldrich) or CHCl$_3$ (99.9% Biosolve) for 100 seconds, typically at pressures of 5×10^{-8} mbar. This dose corresponds to 5 Langmuir (1 Langmuir (L): 1×10^{-6} mbar s) and is roughly equivalent to one monolayer of haloform on the ice surface.

Desorption products were detected using a differentially pumped quadrupole mass spectrometer (QMS Balzers QS 422, sensitive up to 511 AMU). Masses 18 (H$_2$O$^+$), 82.5 (CHCl$_2^+$), 120 (CHCl$_3^+$), 171 (CHBr$_2^+$), and 252 (CHBr$_3^+$) were monitored. We used the CHCl$_2^+$ fragment ($m/z = 82.5$), from CHCl$_3$ dissociated in the QMS, as a probe of molecules desorbed intact from the surface. CHBr$_3$, however, dissociates both on the Pt surface and in the mass spectrometer, and therefore the CHBr$_3^+$ fragment ($m/z = 252$) must be used as a probe of the bromoform molecules desorbing intact from the surface.

In this study, a water ML (monolayer) is defined as the dose of water necessary to form an ice-like bilayer on the substrate, which corresponds to the coverage for which the monolayer TPD peak (at ~170 K) is saturated, and the multilayer peak around 160 K starts to appear [21]. TPD data were typically collected up to substrate temperatures of 650 K, at a heating rate of 0.5 K s^{-1}.

3. Results and discussion

Fig. 1 shows the TPD spectra of CHCl$_3$ dosed on the surfaces of (a) ASW and (b) CI. CHCl$_3$ desorbs at 130 K from the ASW surface (Fig. 1, curve (a)) and at 140 K from the CI surface (Fig. 1, curve (b)). A small shoulder at ~130 K is observed in the case of CI, which is attributed to incomplete crystallization of the water layer. For comparison, the TPD spectrum of CHCl$_3$ from the bare Pt(533) surface is also shown (Fig. 1, curve (c)), exhibiting a broad desorption feature centered around 190 K.

Fig. 1 reveals a significant change in the desorption temperature of CHCl$_3$ with the phase of the underlying ice film. Apparently, CHCl$_3$ adsorbs differently on ASW and CI and appears to be more strongly bound to the CI surface. The difference in desorption kinetics of CHCl$_3$
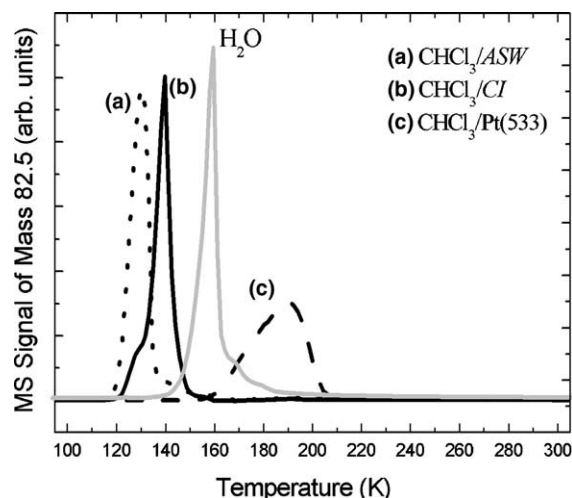

Fig. 1. Desorption of 5 L of CHCl$_3$ adsorbed on the surface of ice: (a) 25 ML of ASW (dotted curve), (b) 16 ML of CI (solid curve), both grown on Pt(533) surface, and (c) bare Pt(533) surface (dashed curve). The gray curve (different scale) indicates the desorption peak of 25 ML of ASW and the bump around 168 K indicates the desorption peak of water monolayer. Heating rate = 0.5 K/s.

have been used previously to distinguish between ASW and CI surfaces [22]. Similar dependencies of desorption temperature on the underlying ice phase have been observed previously for, for example, N$_2$ [23,24] and CHF$_2$Cl [25].

Surprisingly, the desorption of CHBr$_3$ exhibits completely different behavior. Fig. 2 shows the TPD spectra of CHBr$_3$ dosed on the surfaces of (a) ASW, (b) CI, and (c) bare Pt(533). In contrast to CHCl$_3$, if CHBr$_3$ is dosed on either of the ice surfaces (Fig. 2, curves (a) and
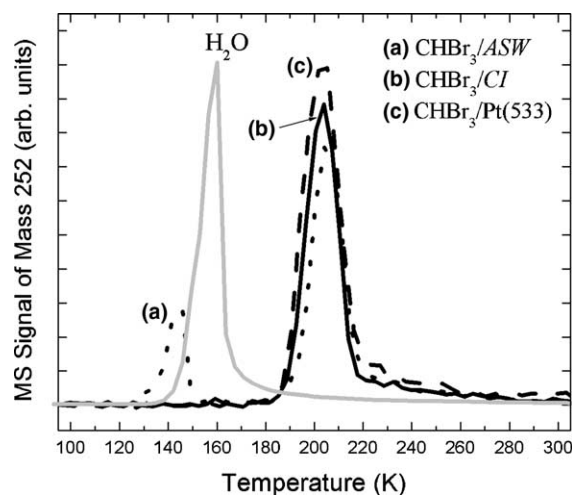

Fig. 2. Desorption of 5 L of CHBr$_3$ adsorbed on the surface of ice: (a) 43 ML of ASW (dotted curve), (b) 35 ML of CI (solid curve), both grown on Pt(533) surface, and (c) bare Pt(533) surface (dashed curve). The gray curve (different scale) indicates the desorption peak of 43 ML of ASW. Heating rate = 0.5 K/s.

(b)), it desorbs predominantly at 204 K, equivalent to the desorption from the bare Pt(5 3 3) surface (Fig. 2, curve (c)). At this temperature, water has completely desorbed from the Pt(5 3 3) substrate. For $CHBr_3$ desorption from ASW, some signal can also be observed at 144 K: with increasing ASW layer thickness, this peak increases in intensity, as the peak at 204 K decreases. In the case of thicker CI layers, some $CHBr_3$ also desorbs from the CI surface, at $\sim$157 K.

These results indicate that the $CHBr_3$ molecules have significant mobility on the ice surfaces, allowing the $CHBr_3$ to cross the ice layer and adsorb directly on the Pt(5 3 3) substrate, displacing the water. The greater stability of $CHBr_3$ on Pt(5 3 3) surface is corroborated by TPD profiles (not shown) from the Pt(5 3 3)/$CHBr_3$/ASW system, where the desorption of the $CHBr_3$ dosed on the bare Pt(5 3 3) surface is unaffected by subsequent exposure to water.

To determine the temperature at which the $CHBr_3$ molecules reach the Pt surface, either during dosing at 85 K or during the TPD measurements, we used RAIRS to trace the location of the $CHBr_3$ molecules during slow heating (0.25 K/s). Fig. 3 (curve (a)) shows the RAIR spectrum of 5 L of $CHBr_3$ deposited at 85 K on a 40 ML ASW covered Pt(5 3 3) substrate. On ASW the C–H stretching vibration of $CHBr_3$, at 3025 cm^{-1}, is slightly shifted from the gas phase peak position (3050 cm^{-1}) [26,27]. This vibration is not visible for $CHBr_3$ adsorbed on bare Pt(5 3 3). Thus, it can be used as a probe of $CHBr_3$ mobility: as soon as the $CHBr_3$ becomes mobile, it will reach the Pt surface, and the CH intensity will disappear. Indeed, as shown in Fig. 3B, the

3025 cm^{-1} peak of $CHBr_3$ on ASW (curve (a)) disappears as amorphous water crystallizes (curve (c)); the change in OH stretch vibration region reflects the crystallization of the water layer. Up to the crystallization temperature, the intensity of the CH peak is constant and identical for varying ASW layer thickness, indicating that the $CHBr_3$ is adsorbed on the outer surface of water layer. Upon crystallization, some $CHBr_3$ desorbs (TPD peak at 144 K in Fig. 2) and the rest diffuses through the layer and adsorbs to the Pt(5 3 3) surface (becoming invisible to RAIRS), even though water desorption is not yet complete. This $CHBr_3$ desorbs at $\sim$204 K from Pt surface. For $CHBr_3$ dosed on the CI surface, no CH signal was observed in the RAIR spectra at 85 K, indicating that, even at this low temperature, $CHBr_3$ already diffuses through the layer to the Pt substrate.

The decisive role of the morphology of the water layer in the $CHBr_3$ diffusion to the Pt substrate is corroborated by TPD measurements with a higher temperature ramp (5 K/s), as shown in Fig. 4. Unlike heating rates of 0.5 K/s, at 5 K/s ASW does not crystallize prior to desorption, evinced by RAIRS measurements. The TPD spectra of $CHBr_3$ dosed on the surfaces of (a) ASW and (b) CI, measured at 5 K/s, are shown in Fig. 4. In contrast to the TPD measured at 0.5 K/s (Fig. 2, curve (a)), all the $CHBr_3$ desorbs before ASW has completely desorbed (at $\sim$173 K – Fig. 4, curve (a)) and never reaches the Pt surface. Conversely, if $CHBr_3$ is dosed onto CI, it desorbs primarily from Pt(5 3 3) substrate, at 236 K (Fig. 4, curve (b)), similar to the TPD results at 0.5 K/s. The *time* integrated intensity
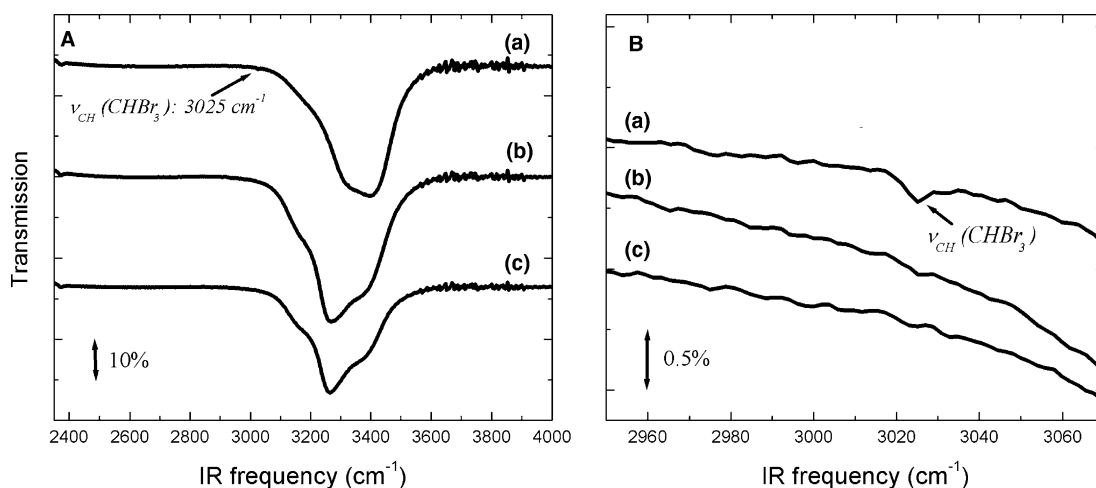

Fig. 3. (A) RAIR spectra of $CHBr_3$ on different types of ice grown on Pt(5 3 3): (a) $CHBr_3$/ASW, (b) $CHBr_3$/(30% ASW + 70%CI), and (c) $CHBr_3$/CI. The RAIR spectra were measured simultaneously with slow heating (0.25 K/s) of 5 L of $CHBr_3$ dosed on 40 ML of ASW at 85 K. In the OH stretching vibration region (2900–3700 cm^{1}), the phase transition from ASW (curve (a)) to CI (curve (c)) is visible. (B) Enlargement of the 2950–3070 cm^{-1} region of the previous RAIR spectra, showing the disappearance, upon ASW crystallization, of the CH vibrational peak of $CHBr_3$ (at 3025 cm^{-1}) on ASW, accompanied by the change in the leading edge of the (large) peak corresponding to the OH stretching vibration. The ASW/CI percentage composition has been determined from the relative contributions of a linear combination of the RAIR spectra of pure ASW and CI [22].
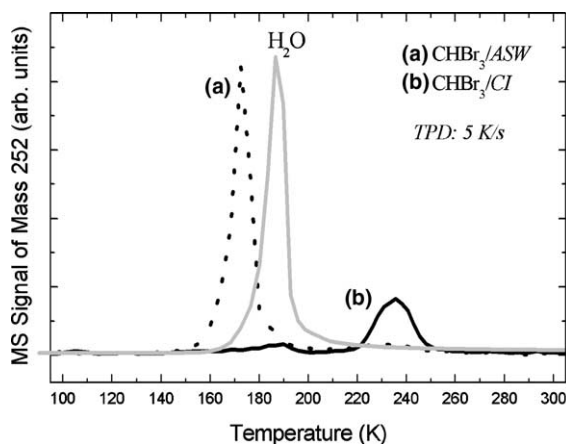
Fig. 4. Desorption of 5 L of CHBr₃ adsorbed on the surface of ice: (a) 65 ML of ASW (dotted curve) and (b) 55 ML of CI (solid curve), both grown on Pt(5 3 3) surface. The gray curve (different scale) indicates the desorption peak of 65 ML of ASW. Heating rate = 5 K/s. High intensity of the TPD peak in curve a is due to the enhanced (partial) dissociation of CHBr₃ on Pt(5 3 3) surface compared to the ice surfaces. See text.

of the $CHBr_3$ desorption from ASW (Fig. 4, curve (a)) is higher than the *time* integrated intensity of the $CHBr_3$ desorption from Pt(533) surface either at 5 K/s (Fig. 4, curve (b)) or 0.5 K/s (Fig. 2, curve (b)). This is due to the fact that the partial dissociation of $CHBr_3$ on Pt(5 3 3) is more pronounced than on ice surfaces. (The $CHBr_3$ peaks shown in Fig. 2, curve (b) and in Fig. 4, curve (b) have same *time* integrated intensity).

The present results clearly indicate that the $CHBr_3$ molecules have significant mobility on CI surfaces, that allows them to percolate through the ice layer, possibly through defects in the ice layer structure, and to adsorb directly on the Pt(5 3 3) substrate. The occurrence of grain boundaries or the formation of fractures during the crystallization of ASW apparently lead to the Pt substrate being exposed to $CHBr_3$ prior to the complete desorption of water. Previously, Smith et al. [28] have shown that, upon crystallization, cracks are formed in the ice layer resulting in a direct connection between substrate and vacuum via which molecules can escape from the substrate in a 'molecular volcano'. For increasing ice thickness, less channels are completely connecting the outer surface with the substrate and therefore less $CHBr_3$ can get to the Pt surface, resulting in the increased intensity of the TPD peak at 144 K in Fig. 2. It is very difficult to envisage a mechanism for $CHBr_3$ percolating the bulk ice, as has been observed for NH_3 and CH_3OH [29], since this requires the formation of $CHBr_3 \cdot xH_2O$ hydrates [29], which, to our knowledge, have not been reported.

In contrast, $CHCl_3$ molecules do not exhibit significant mobility on CI surfaces. Despite the fact that

$CHCl_3$ is a physically smaller molecule than $CHBr_3$, it does not reach the Pt substrate, even though the CI used was identical to that in the $CHBr_3$ experiments. This observation is consistent with recent investigations reporting the absence of surface mobility of $CDCl_3$ on CI surface, between 130 and 160 K [29]. This was surmised to be due to either $CDCl_3$ being incorporated into the bulk of the CI layer or island formation [29]. Our results clearly demonstrate that $CHCl_3$ adsorbs only on the outer surface of the ice layers. TPD spectra (not shown) from $CHCl_3$ purposely introduced into the ice layer (in so-called 'sandwich' experiments) look markedly different.

Our results indicate a markedly lower barrier for surface diffusion of $CHBr_3$ on ice compared to $CHCl_3$. This is somewhat surprising, since the $CHBr_3$ seems slightly more strongly bound, as evidenced by its higher desorption temperature. The binding strength is determined by the polarizability (dipole-induced dipole interaction; larger for $CHBr_3$), the dipole moment (dipole-dipole interaction; larger for $CHCl_3$) and the hydrogen-bonding interaction of the halogen atom (it is known that the haloform molecules interact with the ice surface through their halogen atom [14]) with the free O–H groups (larger for $CHCl_3$). Apparently, the sum of these contributions for the coordinate perpendicular to the surface (i.e. the desorption coordinate) is such that the $CHBr_3$–water interaction is stronger than the $CHCl_3$–water interaction. Clearly, for the coordinate parallel to the surface (the diffusion coordinate) the same contributions play a role, but apparently in a different manner, as $CHBr_3$ is more mobile. It may also be that additional contributions play a role for the diffusion process, such as the stronger repulsion between the more electronegative Cl atoms and water oxygen atoms, inhibiting diffusion as Cl atoms have to move over negative oxygen atoms. In addition, the ~10% smaller chloroform molecules may fit more deeply into the hexagonal shafts of the ice structure so that diffusion could be sterically hindered.

4. Conclusions

We report that $CHBr_3$ molecules exhibit surface diffusion on the surface of crystalline ice, even at temperatures as low as 85 K. $CHCl_3$ molecules remain immobile on CI surfaces until they desorb (around 140 K).

The observed trends in the surface mobility of these small organic molecules on ice surfaces should be helpful to further understanding certain chemical phenomena of atmospheric relevance. The anomalous reactivity of bromine containing species in atmospheric chemistry [2], particularly in heterogeneous processes related to ozone depletion [30–33], may well be related to the high mobility of these species on ice surfaces.

Acknowledgements

References

[1] T. Tang, J.C. McConnel, Geophys. Res. Lett. 23 (1996) 2633.
[2] WMO, Scientific Assessment of Ozone Depletion: 1994 (WMO, 1995).
[3] R.R. Garcia, S. Solomon, J. Geophys. Res. Atmos. 99 (1994) 12937.
[4] S. Solomon, M. Mills, L.E. Heidt, W.H. Pollock, A.F. Tuck, J. Geophys. Res. Atmos. 97 (1992) 825.
[5] W.T. Sturges, G.F. Cota, P.T. Buckley, Nature 358 (1992) 660.
[6] L.J. Carpenter, P.S. Liss, J. Geophys. Res. Atmos. 105 (2000) 20539.
[7] P.D. Nightingale, G. Malin, P.S. Liss, Limnol. Ocean. 40 (1995) 680.
[8] W.T. Sturges, D.E. Oram, L.J. Carpenter, S.A. Penkett, A. Engel, Geophys. Res. Lett. 27 (2000) 2081.
[9] J.E. Nielsen, A.R. Douglass, J. Geophys. Res. Atmos. 106 (2001) 8089.
[10] W.S. McGivern, O. Sorkhabi, A.G. Suits, A. Derecskei-Kovacs, S.M. North, J. Phys. Chem. A 104 (2000) 10085.
[11] J.T. Roberts, Acc. Chem. Res. 31 (1998) 415.
[12] J.E. Schaff, J.T. Roberts, J. Phys. Chem. 100 (1996) 14151.
[13] J.E. Schaff, J.T. Roberts, Surf. Sci. 426 (1999) 384.
[14] N.S. Holmes, J.R. Sodeau, J. Phys. Chem. A 103 (1999) 4673.
[15] B. Riedmüller, F. Giskes, D.G.v. Loon, P. Lassing, A.W. Kleyn, Meas. Sci. Technol. 13 (2002) 141.
[16] H.G. Jenniskens, A. Bot, P.W.F. Dorlandt, W.v. Essenberg, E.v. Haas, A.W. Kleyn, Meas. Sci. Technol. 8 (1997) 1313.
[17] H. Wang, R.G. Tobin, C.L. DiMaggio, G.B. Fisher, D.K. Lambert, J. Chem. Phys. 107 (1997) 9569.
[18] J.E. Schaff, J.T. Roberts, J. Phys. Chem. 98 (1994) 6900.
[19] J.E. Schaff, J.T. Roberts, Langmuir 14 (1998) 1478.
[20] S. Haq, J. Harnett, A. Hogdson, J. Phys. Chem. B 106 (2002) 3950.
[21] R.S. Smith, Z. Dohnálek, G.A. Kimmel, K.P. Stevenson, B.D. Kay, Chem. Phys. 258 (2000) 291.
[22] E.H.G. Backus, M.L. Grecea, A.W. Kleyn, M. Bonn, submitted.
[23] Z. Dohnálek, R.L. Ciolli, G.A. Kimmel, K.P. Stevenson, R.S. Smith, B.D. Kay, J. Chem. Phys. 110 (1999) 5489.
[24] Z. Dohnálek, G.A. Kimmel, R.L. Ciolli, K.P. Stevenson, R.S. Smith, B.D. Kay, J. Chem. Phys. 112 (2000) 5932.
[25] D.J. Safarik, R.J. Meyer, C.B. Mullins, J. Vac. Sci. Technol. A 19 (2001) 1537.
[26] R. Venkatraman, J.S. Kwiatkowski, G. Bakalarski, J. Leszczynski, Molec. Phys. 98 (2000) 371.
[27] E.E. Rogers, S. Sabramowitz, M.E. Jacox, D.E. Miligan, J. Chem. Phys. 52 (1970) 2198.
[28] R.S. Smith, C. Huang, E.K.L. Wong, B.D. Kay, Phys. Rev. Lett. 79 (1997) 909.
[29] F.E. Livingston, J.A. Smith, S.M. George, J. Phys. Chem. A 106 (2002) 6309.
[30] R.P. Wayne, G. Poulet, P. Biggs, J.P. Burrows, R.A. Cox, P.J. Crutzen, G.D. Hayman, M.E. Jenkin, G.L. Bras, G.K. Moortgat, U. Platt, R.N. Schindler, Atmos. Environ. 29 (1995) 2677.
[31] J.G. Anderson, W.H. Brune, S.A. Lloyd, D.W. Toohey, S.P. Sander, W.L. Starr, M. Loewenstein, J.R. Podolske, J. Geophys. Res. Atmos. 94 (1989) 11480.
[32] M.B. McElroy, R.J. Salawitch, S.C. Wofsy, J.A. Logan, Nature 321 (1986) 759.
[33] S. Solomon, R.W. Sanders, H.L. Miller, J. Geophys. Res. Atmos. 95 (1990) 13807.